NJC

Cite this: New J. Chem., 2012, **36**, 723–731

www.rsc.org/njc

PAPER

Ln(III)-cored complexes based on boron dipyrromethene (Bodipy) ligands for NIR emission†

Jung Ho Ryu,[a] Yu Kyung Eom,[a] Jean-Claude G. Bünzli*[ab] and Hwan Kyu Kim*[a]

Received (in Montpellier, France) 10th September 2011, Accepted 23rd November 2011
DOI: 10.1039/c2nj20786a

Two Bodipy-based chromophores have been synthesized, which bear two methoxyphenyl substituents in the 1,7 positions and either hydrogen (**L1**) or bromine (**L2**) atoms in the 2,6 positions, with the aim of testing their ability to sensitize the luminescence of near-infrared emitting $\mathrm{Ln^{III}}$ ions. Despite the presence of the two halogen substituents in **L2**, the two chromophores display very similar absorption and emission properties, the only difference being a drop in the quantum yield from 31% for **L1** to 21% for **L2**. In addition, no triplet state emission could be evidenced for both chromophores as well as for their tris complexes with $\mathrm{Gd^{III}}$ ions. This is traced back to unfavorable conformation of the molecule, preventing efficient intersystem crossing. Complexes with stoichiometry $[\mathrm{Ln}(\mathbf{L}i)_3(\mathrm{tpy})]$ have been isolated for Ln = Gd, Er, Yb and fully characterized. Ligand emission is partially quenched (20–40%) in the $\mathrm{Er^{III}}$ and $\mathrm{Yb^{III}}$ complexes and typical metal-centred luminescence is detected at 1530 ($\mathrm{Er^{III}}$) and 978 ($\mathrm{Yb^{III}}$) nm upon excitation in the orange portion of the visible spectrum (583 nm). In these complexes, the main energy transfer pathway involves the singlet state(s) of the ligands: the lowest $^1\pi\pi$ state emission overlaps the $\mathrm{Er}(^4\mathrm{F}_{9/2} \leftarrow {}^4\mathrm{I}_{15/2})$ absorption band and the $^1\pi\pi$–$\mathrm{Yb}(^2\mathrm{F}_{5/2})$ gap amounts to only 5700 cm^{-1}. This study demonstrates that the Bodipy framework is adequate for sensitizing the luminescence of NIR-emitting lanthanide ions, allowing excitation wavelengths extending into the orange portion of the visible spectrum and yielding complexes with large molar absorption coefficients ($\log \varepsilon \approx 5.0$–$5.2$). Additionally it also points to the importance of the conformation of the chromophores on the yield of intersystem crossing.

Introduction

Luminescent lanthanide complexes with organic ligands are attracting much attention because of their fundamental scientific importance and potential utility in a wide variety of photonic applications, such as planar waveguide amplifiers, plastic lasers, light-emitting diodes, luminescent probes and solar cells.[1–7] In particular, the development of planar waveguides integrating optical amplifiers with wavelength division multiplexing (WDM) devices based on $\mathrm{Er^{III}}$ emission is recognized to be essential for successfully realizing high-speed communication photonic systems. However, there are several problems that still impede the use of existing materials in real planar waveguide optical amplifiers. At present, $\mathrm{Er^{III}}$-doped silica materials are being used widely. However, the forbidden $4f^n$–$4f^n$ electronic transitions and the poor solubility of $\mathrm{Er^{III}}$ ions in conventional inorganic media lead to yet unsatisfactory amplification properties.[5]

One way to remedy this problem is to take advantage of the large absorption coefficients of organic ligands and their ability to sensitize lanthanide NIR luminescence.[8–10] The sensitization process is much more effective than direct f–f excitation. Until now, a major factor in this process has often been identified as being the triplet state(s) of the ligands. As a consequence many research studies aiming at finding efficient sensitizers for lanthanide NIR luminescence follow the trends for visible-luminescence sensitization and are focused on identifying luminescent ligands with a triplet state matching the energies of the receiving lanthanide ion levels.[11–13]

Interestingly, however, it is known for a long time that energy transfer from excited singlet state(s) to $\mathrm{Ln^{III}}$ ions can also be effective,[14] particularly for fluorescent lanthanide ions, and this mechanism starts now to be fully recognized.[15–17] Other important donor states for sensitizing lanthanide luminescence include intraligand charge transfer states (ILCT) which are given more attention presently.[18–21] In our laboratory,

---

[a] *Department of Advanced Materials Chemistry and WCU Center for Next Generation Photovoltaic Systems, Korea University, Jochiwon, Chungnam 339-700, Republic of Korea.*
E-mail: hkk777@korea.ac.kr; Fax: +82-41-860-1493;
Tel: +82-41-860-1493
[b] *École Polytechnique Fédérale de Lausanne, Institute of Chemical Sciences and Engineering, BCH 1402, CH-1015 Lausanne, Switzerland. E-mail: jean-claude.bunzli@epfl.ch*

† Electronic supplementary information (ESI) available: ^{1}H-NMR spectrum, ^{13}C-NMR spectrum, ^{19}F-NMR spectrum, EI-mass spectrum, thermogravimetric analysis and photophysical data (time-resolved spectroscopy and excitation spectra). See DOI: 10.1039/c2nj20786a

we have long been interested in deciphering energy transfer pathways in various lanthanide complexes, demonstrating for example (i) the role of the triplet state of metallo (Zn^{II}, Pt^{II}) porphyrin units in sensitizing Er^{III} luminescence in macrocyclic and dendrimeric complexes,[22] (ii) singlet state excitation of the same ion through anthracene units,[23,24] and (iii) the atypical excitation pathway through ILCT states involving dansyl (Nd^{III}, Er^{III})[17] and naphthalene (Eu^{III})[20] units. In view of the complexity in the energy transfer processes from the ligand(s) to the lanthanide ions, which may involve several different mechanisms and states, it is therefore important to determine which is the most influential energy transfer path in a given system.

In this paper, we turn our attention to 4,4-difluoro-4-bora-3*a*,4*a*-diaza-*s*-indacene (boron dipyrromethene or Bodipy) chromophores which are photostable dyes used in tunable dye lasers,[24] biological labelling,[26] singlet oxygen production for photodynamic treatment (PDT) of cancer,[27] and, more recently, in heterojunction dye sensitized solar cells[28] as well as for solar hydrogen production.[29] These dyes feature high thermal and photochemical stability, large fluorescence quantum yields and negligible triplet-state formation.[25] The yield of inter-system crossing can however be considerably enhanced upon bromination of the 2,6 positions,[29] which makes this framework interesting for exploring the relative importance of the triplet *versus* singlet state sensitization paths in luminescent lanthanide complexes. To this end, we have designed and synthesized the un-substituted and the dibrominated ligands **L1** and **L2** (Scheme 1) which form neutral tris complexes with Ln^{III} ions (Ln = Gd, Er, and Yb). Saturation of the coordination sphere is conveniently achieved with terpyridine (tpy) and the photophysical parameters of both ligands and their ternary complexes are investigated and discussed.

Experimental

General

Reagents were purchased from Sigma-Aldrich, Fluka Inc., TCI Co., or Junsei Inc. and were used as received. Tetrahydrofuran (THF) was freshly distilled from sodium-benzophenone under N_2 atmosphere. Diethyl ether and CH_2Cl_2 were freshly distilled from CaH_2 under N_2 atmosphere.

^1H-, ^{13}C- and ^{19}F-NMR spectra were recorded using a Varian Oxford 300 MHz spectrometer; chemical shifts are reported in ppm with respect to tetramethylsilane or hexafluorobenzene as internal standard. Elemental analysis was performed by the Center for microanalysis of KAIST (Daejeon) with a EA1110-FISONS elemental analyzer manufactured by ThermoQuest Italia S.P.A (accuracy: 0.3%). Lanthanide content was determined by atomic emission spectroscopy with a ELAN 6100 ICP-MS spectrometer from Perkin-Elmer-Sciex; experiments were carried out at Seoul National University. Thermogravimetric

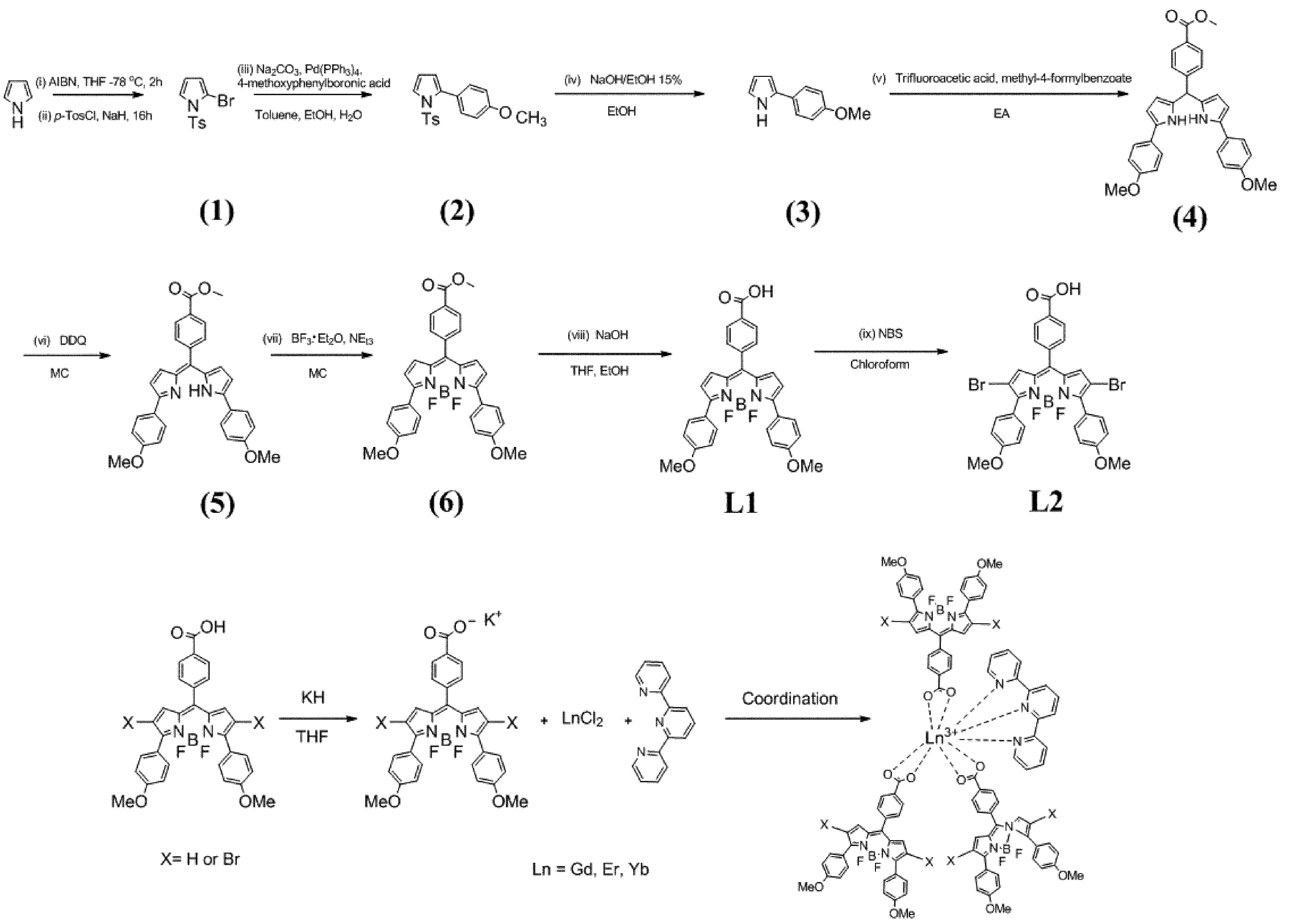

Scheme 1 Schematic diagram for the synthesis of the Bodipy ligands and their complexes.

analysis was performed on a TGA N-1000 with a heating rate of 10 °C min^{-1} under N_2 atmosphere. Infrared spectra were measured on KBr pellets using a Jasco FT/IR-4200 Spectrometer. MALDI-TOF mass spectrometry was performed on a Voyager-DETM STR Biospectrometry TM workstation from PerSeptive Biosystems. Absorption spectra were recorded with a Shimadzu UV-2401PC spectrophotometer and photoluminescence spectra with a Fluorolog FL-3-22 fluorometer from Horiba-Jobin-Yvon Ltd. equipped with a 450 W Xe-lamp and two analyzing monochromators. Visible emission spectra were detected with a Hamamatsu R928 photomultiplier while near-IR emission spectra were measured with the Peltier-cooled Hamamatsu H9170-75 photomultiplier system. Solutions were saturated with N_2 to avoid the quenching effect of dioxygen. Lifetime measurements were performed with an excitation at 583 nm by using a Horiba Jobin Yvon iHR320 Spectrometer. The excitation beam had a 100 ps pulse width at 1 MHz repetition rate. The emission signal was analyzed in time-correlated single photon counting mode.

Optimized geometry of the ligand have been performed by a semi-empirical method at AM1 level with Hyperchem 7.5 professional while interpretations of the ligand absorption spectra are based on calculations with Scigress Explorer Ultra Version 7.7.

Synthesis of Bodipy ligands

2-Bromo-1-tosyl-1*H*-pyrrole (1). 1,3-Dibromo-5,5-dimethylhydantoin (6.53 g, 22.4 mmol) was added to a solution of 3.1 mL of pyrrole (44.7 mmol) in 120 mL of freshly distilled THF in a dried flask under N_2 atmosphere at −78 °C. The mixture was stirred for 30 min and allowed to stand for an additional 3.5 h at −78 °C. To this solution were added 4 mL of Bu_3N and 180 mL of distilled Et_2O and the mixture was stirred for 10 min at −78 °C. The resulting gray precipitate was removed by filtration and the solution was concentrated to remove Et_2O. *p*-Toluenesulfonyl chloride (17.04 g, 89.4 mmol) was then added and the inert atmosphere was reestablished. The solution was cooled to 0 °C and 5.36 g (134.0 mmol) of NaH (60% in mineral oil) was added. The mixture was stirred for 18 h and 60 mL of H_2O was added. The mixture was extracted with Et_2O and the ether extracts were washed with successive portions of 1 M HCl and $NaHCO_3$. This mixture was combined with an equal volume of 2 M NaOH and was stirred for 2 h at room temperature The layers were separated and the organic extract was washed with H_2O and 2 M NaOH. The organic layer was dried over $MgSO_4$ and concentrated to give a light brown solid. Recrystallization from isopropyl alcohol gave (**1**) in 23% yield. ^{1}H-NMR (300 MHz, $CDCl_3$) = 2.43 (s, 3H), 6.23–6.29 (m, 2H), 7.32 (d, *J* = 8.3 Hz, 2H), 7.46 (dd, *J* = 2.0, 3.5 Hz, 1H) and 7.81(d, *J* = 8.4 Hz, 2H).

2-(4-Methoxyphenyl)-1-tosyl-1*H*-pyrrole (2). A mixture of (**1**) (10 g, 33.31 mmol), 4-methoxyphenylboronic acid (6 g, 39.48 mmol), $Pd(PPh_3)_4$ (1.8 g, 1.56 mmol), 30 mL of toluene, 30 mL of EtOH, and 30 mL of 2 M Na_2CO_3 was refluxed at 100 °C for 24 h under N_2 atmosphere and was extracted with ethyl acetate. The organic layer was washed with brine and water and dried over $MgSO_4$, filtered and concentrated *in vacuo*. The crude product was purified by recrystallization from isopropyl alcohol to give (**2**) as a white crystalline solid in 70% yield. ^{1}H-NMR (300 MHz, $CDCl_3$) = 2.34 (s, 3H), 3.84 (s, 3H), 6.10 (dd, *J* = 1.8, 3.0 Hz 1H), 6.28 (t, *J* = 3.4 Hz 1H), 6.81–6.86 (m, 2H), 7.09–7.17 (m, 4H), 7.25–7.26 (m, 2H) and 7.41 (dd, *J* = 1.8, 3.1 Hz 1H).

2-(4-Methoxyphenyl)-1*H*-pyrrole (3). A mixture of 0.050 g (0.15 mmol) of (**2**) in 0.6 mL of EtOH and 0.2 mL of 15% ethanolic NaOH was stirred at reflux temperature for 3 h. The solution was concentrated *in vacuo* and the residue was dissolved in CH_2Cl_2 and washed with H_2O. The organic layer was dried over $MgSO_4$ and concentrated *in vacuo* to give 0.025 g of (**3**) as a white solid, in 95% yield. ^{1}H-NMR (300 MHz, $CDCl_3$) = 3.81 (s, 3H), 6.27 (dd, *J* = 2.8, 5.7 Hz 1H), 6.40 (t, *J* = 3.5 Hz, 1H), 6.79 (dd, *J* = 2.4, 3.9 Hz 1H), 6.88–6.91 (m, 2H), 7.36–7.39 (m, 2H) and 8.32 (br s, 1H).

Methyl-4-(bis(5-(4-methoxyphenyl)-1*H*-pyrrole-2-yl)methyl) benzoate (4). A mixture of 1.82 g (10.51 mmol) of (**3**), 0.69 g (4.2 mmol) of methyl 4-formylbenzoate, and 20 mL of ethyl acetate was added to a 250 mL 3-necked round bottomed flask and degassed with N_2 atmosphere for 5 min. Trifluoroacetic acid (0.03 mL, 0.42 mmol) was then added all at once. The solution was stirred under N_2 atmosphere at room temperature for 1 h. Then, 50 mL of 0.1 N NaOH was added to the solution. The solution was extracted with ethyl acetate. The organic layer was washed with brine and water, dried over $MgSO_4$, filtered, and concentrated *in vacuo*. The crude product was purified by recrystallization from the hexane/CH_2Cl_2 mixture to give a violet solid in 61% yield. ^{1}H-NMR (300 MHz, $CDCl_3$) = 3.80 (s, 6H), 3.91 (s, 3H), 5.58 (s, 1H), 5.93 (s, 2H), 6.33 (s, 2H), 6.88 (d, *J* = 8.4 Hz, 4H), 7.32 (d, *J* = 8.4 Hz, 4H), 7.38 (d, *J* = 8.1 Hz, 2H), 8.01 (d, *J* = 8.4 Hz, 2H) and 8.15 (s, 2H).

(*Z*)-Methyl 4-((5-(4-methoxyphenyl)-1*H*-pyrrole-2-yl)-(5-(4-methoxyphenyl)-2*H*-pyrrole-2-ylidene)methyl)benzoate (5). 2,3-Dichloro-5,6-dicyano-1,4-benzoquinone (0.4 g, 1.76 mmol) was added to a solution of 0.6 g (1.12 mmol) of (**4**) in 50 mL CH_2Cl_2. The mixture was stirred at room temperature for 1 h. The solution was concentrated *in vacuo*. The crude product was purified by flash column chromatography (silica, hexane/ethyl acetate). Yield: 23%. ^{1}H-NMR (300 MHz, $CDCl_3$) = 3.90 (s, 6H), 3.98 (s, 3H), 6.61 (d, *J* = 4.2 Hz, 2H), 6.77 (d, *J* = 4.2 Hz, 2H), 7.03 (d, *J* = 9.0 Hz, 4H), 7.62 (d, *J* = 8.1 Hz, 2H), 7.86 (d, *J* = 8.4 Hz, 4H) and 8.131 (d, *J* = 7.8 Hz, 2H).

Boron dipyrromethene (6). A solution of 0.24 g (0.49 mmol) of (**5**) and 0.12 g (1.10 mmol) of triethylamine in 30 mL of dried CH_2Cl_2 was stirred under N_2 atmosphere at room temperature for 10 min. Then, boron trifluoride diethyl etherate (0.3 mL, 2.47 mmol) was added dropwise over 10 min. The resulting solution was stirred for 24 h at room temperature and the crude product was purified by flash column chromatography (silica, hexane/CH_2Cl_2). Yield: 42%. ^{1}H-NMR (300 MHz, $CDCl_3$) = 3.85 (s, 6H), 3.99 (s, 3H), 6.62 (d, *J* = 4.2 Hz, 2H), 6.78 (d, *J* = 4.5 Hz, 2H), 6.96 (d, *J* = 9.0 Hz, 4H), 7.65 (d, *J* = 8.1 Hz, 2H), 7.88 (d, *J* = 9.0 Hz, 4H) and 8.18 (d, *J* = 8.4 Hz, 2H).

Bodipy–CO_2H (L1). A solution of ethanolic NaOH (0.85 g, 21 mmol) was added to a stirred solution of 0.2 g (0.37 mmol) of (**6**) in THF/EtOH. The solution was stirred at room temperature overnight. The solution was concentrated *in vacuo*. The crude product was purified by flash column chromatography (silica, CH_2Cl_2/MeOH), and then the product was acidified to pH 4 with a solution of HCl (1 M). The water layer was extracted three times with ethyl acetate. The organic phase was dried over $MgSO_4$, filtered and concentrated *in vacuo*. The crude product was purified by recrystallization from the hexane/CH_2Cl_2 mixture to give a green solid. **Bodipy–CO_2H**: Yield: 60%. Anal. calcd. for $C_{30}H_{23}BF_2N_2O_4$: C (68.72%), H (4.42%), N (5.34%); found: C (68.41%), H (4.46%), N (5.10%); ^{1}H-NMR (300 MHz, $CDCl_3$) = 3.86 (s, 6H), 6.64 (d, *J* = 3.6 Hz, 2H), 6.77 (d, *J* = 3.5 Hz, 2H), 6.95 (d, *J* = 9.0 Hz, 4H), 7.70 (d, *J* = 8.1 Hz, 2H), 7.89 (d, *J* = 9.0 Hz, 4H) and 8.26 (d, *J* = 7.8 Hz, 2H); ^{13}C-NMR (226.4 MHz, DMSO) = 166.82, 160.5, 155.8, 142.5, 136.4, 133.4, 131.8, 131.7, 130.9, 129.5, 121.7, 114.1, 113.4, 109.6, 55.2; ^{19}F-NMR (282.3 MHz, DMSO) = −137.5 (s, 2F), MS (MALDI-TOF): *m*/*z* 524.06 (M^+), calc. 524.17.

Br-Bodipy-CO_2H (L2). A mixture of L1 (0.1 g, 0.19 mmol), NBS (0.075 g, 0.42 mmol), AIBN (0.004 g, 0.02 mmol) and 20 mL of CH_3Cl solution was refluxed at 100 °C for 24 h under N_2 atmosphere. The crude product was purified by flash column chromatography (silica, CH_2Cl_2/MeOH), and then the product was acidified to pH 4 with a solution of HCl (1 M). The water layer was extracted with ethyl acetate three times. The organic phase was dried over $MgSO_4$, filtered and concentrated *in vacuo*. The crude product was purified by recrystallization from the hexane/CH_2Cl_2 mixture to give a green solid. **Br–Bodipy–CO_2H**: Yield: 61%. Anal. calcd. for $C_{30}H_{21}BBr_2F_2N_2O_4$: C (52.82%), H (3.10%), N (4.11%); found: C (52.62%), H (3.50%), N (4.00%). ^{1}H-NMR (300 MHz, $CDCl_3$) = 3.85 (s, 6H), 6.92 (m, 6H), 7.62 (d, *J* = 9.0 Hz, 4H), 7.68 (d, *J* = 8.1 Hz, 2H) and 8.27 (d, *J* = 7.8 Hz, 2H); ^{13}C-NMR (226.4 MHz, DMSO) 166.8, 160.6, 157.9, 140.8, 137.7, 135.4, 132.3, 131.0, 130.8, 130.7, 129.3, 124.3, 121.4, 113.9, 55.4; ^{19}F-NMR (282.3 MHz, DMSO) = −139.5. MS (MALDI-TOF): *m*/*z* = 681.87 (M^+), calc. 681.99.

General procedure for the synthesis of [Ln(L*i*)(terpy)] (Ln = Gd, Er, Yb; *i* = 1, 2). A mixture of **L***i* (*i* = 1 or 2; 3 equiv.) and KH (3.3 equiv.) was stirred overnight in freshly distilled THF at room temperature until no more H_2 gas was generated. After the completion of the reaction, a methanol solution of anhydrous $LnCl_3$ (Ln = Gd, Er, or Yb; 1 equiv.) and terpyridine (tpy, 1.1 equiv.) was added to the reaction mixture, and the resulting solution was stirred for 2 days. Subsequently, the resulting solution was filtered, the solvents were removed and the obtained colored solid was washed sequentially with methanol, yielding a dark blue solid.

[Gd(L1)$_3$(tpy)]. Yield: 70%. FT-IR (KBr) [cm^{-1}]: 2932, 1603, 1559, 1469, 1428, 1263, 1217, 1181, 1142.62, 1067, 838, 796, 737, 625, and 546. Anal. calcd. for $C_{105}H_{77}B_3GdF_6N9O_{12}$: C (64.33%), H (3.96%), N (6.43%), Gd (8.02%); found: C (64.93%), H (3.92%), N (6.70%), Gd (8.10%).

[Er(L1)$_3$(tpy)]. Yield: 25%. FT-IR (KBr) [cm^{-1}]: 2927, 1604, 1560, 1469, 1431, 1385, 1262, 1218, 1182, 1144, 1067, 834, 785, 732, 624, and 541. Anal. calcd. for $C_{105}H_{77}B_3ErF_6N_9O_{12}$: C (64.00%), H (3.94%), N (6.40%), Er (8.49%); found: C (63.30%), H (3.72%), N (6.53%), Er (8.53%).

[Yb(L1)$_3$(tpy)]. Yield: 69%. FT-IR (KBr) [cm^{-1}]: 2975, 1604, 1558, 1469, 1428, 1263, 1181, 1142, 1066, 835, 797, 736, and 626. Anal. calcd. for $C_{105}H_{77}B_3YbF6N_9O_{12}$: C (63.81%), H (3.93%), N (6.38%), Yb (8.76%); found: C (64.20%), H (4.02%), N (6.58%), Yb (8.60%).

[Er(L2)$_3$(tpy)]. Yield 38%. FT-IR (KBr) [cm^{-1}]: 2928, 2372, 1667, 1555, 1459, 1427, 1293, 1256, 1225, 1179, 1144, 1067, 833, 734, and 628. Anal. calcd. for $C_{105}H_{71}B_3Br_6ErF_6N_9O_{12}$: C (51.60%), H (2.93%), N (5.16%), Er (6.84%); found: C (51.01%), H (2.97%), N (4.98%), Er (6.92%).

[Yb(L2)$_3$(tpy)]. Yield 65%. FT-IR (KBr) [cm^{-1}]: 2926, 2375, 1606, 1554, 1459, 1427, 1293, 1256, 1224, 1179, 1144, 1067, 990, 907, 832, 744, 693, and 627. Anal. calcd. for $C_{105}H_{71}B_3Br_6YbF_6N_9O_{12}$: C (51.48%), H (2.92%), N (5.15%), Yb (7.06%); found: C (52.10%), H (2.85%), N (5.25%), Yb (7.12%).

[Gd(L2)$_3$(tpy)]. This complex was prepared in the same manner above and a dark blue solid was obtained with a yield of 42%. FT-IR (KBr) [cm^{-1}]: 2961, 2370, 1606, 1554, 1459, 1426, 1292, 1257, 1224, 1178, 1144, 1067, 831, 744, and 627. Anal. calcd. for $C_{105}H_{71}B_3Br_6GdF_6N_9O_{12}$: C (51.82%), H (2.94%), N (5.18%), Gd (6.46%); found: C (51.40%), H (3.01%), N (5.29%), Gd (6.53%).

Results and discussion

Synthesis and characterization

The synthesis of the ligands and of the targeted complexes [Ln(**L1**)$_3$(tpy)] and [Ln(**L2**)$_3$(tpy)] (Ln = Gd, Er, Yb) is depicted in Scheme 1. Intermediate compound (**1**) was prepared by treatment of pyrrole with 1,3-dibromo-5,5-dimethylhydantoin in the presence of AIBN followed by amine protection with *p*-toluenesulfonyl chloride. Reaction of (**1**) with 4-methoxyphenylboronic acid under conditions of the Suzuki cross-coupling reaction yielded (**2**). After protection of the tosyl group with 15% ethanolic NaOH in ethanol,[30] the resulting intermediate (**3**) was reacted with methyl 4-formylbenzoate to obtain (**4**), the oxidation of which was achieved by 2,3-dichloro-5,6-dicyano-1,4-benzoquinone (DDQ), a stronger reactant than 1,4-benzoquinone. The reaction proceeded smoothly but separating the highly colored compound by column chromatography was difficult, which explains the somewhat low yield of this step. The oxidized compound (**5**) was then treated with boron trifluoride etherate in the presence of triethylamine in dried CH_2Cl_2 at room temperature to produce the precursor Bodipy (**6**). The ester group was hydrolyzed in the presence of sodium hydroxide to yield ligand **L1**. Further bromination at the 2 and 6 positions led to the second ligand **L2**. The ligands were characterized by elemental analysis, FT-IR, ^{1}H- ^{13}C-, and ^{19}F-NMR spectra (Fig. S1–S6 in ESI†) MALIDO-TOF mass spectrometry (Fig. S7 and S8 in ESI†), absorption, and emission spectroscopies. Thermogravimetric analyses show the ligands being devoid of solvation water molecules (Fig. S9 in ESI†).

Novel lanthanide-cored complexes with Bodipy ligands were synthesized by a ligand exchange reaction developed in

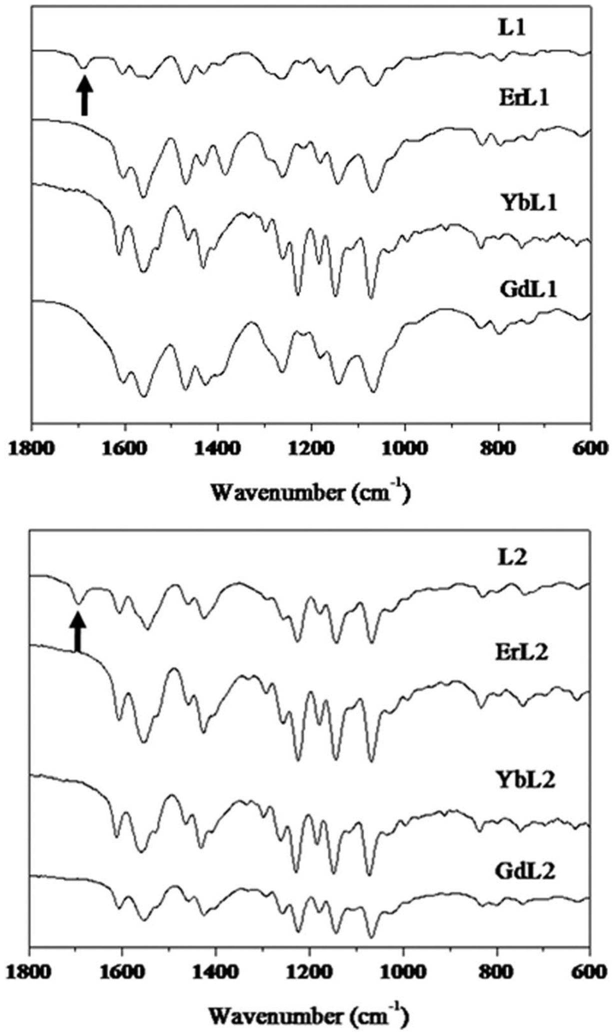

Fig. 1 FT-IR spectra of Bodipy ligands and the corresponding [Ln(**L***i*)$_3$(tpy)] complexes. The arrow points to the C=O stretching vibration of the carboxylic acid function.

our laboratory, starting from anhydrous LnCl$_3$ (Ln = Gd, Er, Yb), and were obtained in 25 ~ 70% yields. The FT-IR spectra of the free ligands exhibit a band at around 1690–1695 cm^{-1} assigned to the carbonyl stretching of conjugated carboxylic acid. All of the vibrational spectra of the Ln-cored complexes are similar and are devoid of this vibration. Instead, the two characteristic bands of asymmetric (*ca.* 1560 cm^{-1}) and symmetric (*ca.* 1430 cm^{-1}) stretching vibration modes of the carboxylate group appear, the latter being mixed with C–C stretching,[31] which explains the presence of a similar, although less intense band in the spectrum of the ligand (Fig. 1 and Fig. S10 in ESI†). These data are indicative of the conversion of the carboxylic acid group into a carboxylate anion as a result of the formation of the Ln-cored complexes.[32,33] The proposed composition of the [Ln(**L***i*)$_3$(tpy)] complexes is further substantiated by elemental analysis including metal content determination.

Ligand-centred photophysical properties

Table 1 Optical properties of the ligands and their complexes in THF at room temperature

Compound	λ_{abs}/nm	ε/M^{-1} cm^{-1}	λ_{em}/nm	ϕ_F^{a}	I_{int}^{b}
L1	583	52 400 ± 3500	622	0.31	1.00
	400	11 450 ± 800			
L1Gd	583	110 300 ± 3270	620		0.98
L1Er	583	121 200 ± 4650	621		0.74
L1Yb	583	122 400 ± 1200	620		0.70
L2	584	56 100 ± 2100	624	0.21	1.00
	409	13 200 ± 500			
L2Gd	584	159 800 ± 5800	626		0.92
L2Er	584	166 600 ± 8400	625		0.63
L2Yb	584	147 400 ± 4200	625		0.76

[a] Measured with respect to chlorophyll A (ϕ_F = 0.32 in dimethylether);[36] estimated accuracy: ±10%. [b] Relative integrated intensity; estimated error: ±5%.

The photophysical parameters for the electronic spectra of the ligands and their complexes are listed in Table 1. The absorption spectrum of ligand **L1** in THF (Fig. 2) exhibits an intense $S_0 \rightarrow S_1$ (π–π^*) transition (log ε = 4.72) centered at λ_{max} = 583 nm and mainly originating from the central core of the ligand. An additional, much weaker band (log ε = 4.06) is seen at 400 nm; it contains a contribution from an intra-ligand charge transfer (ILCT) between the methoxyphenyl groups and the central aromatic system of the ligand. A third band located at about 310 nm, at the limit of the cutoff wavelength of the solvent, corresponds to transitions on the phenyl moieties.[34] Similar absorption bands are observed for ligand **L2**. In line with the bromination of the methoxyphenyl moieties, the main absorption remains almost unshifted, while the second one sustains a bathochromic shift of 9 nm; both transitions display negligible change in molar absorption coefficients with respect to **L1**. Finally, the more energetic absorption is not affected with respect to its energy, but its intensity is smaller.

Upon excitation at the absorption maximum, the photoluminescence spectrum of ligand **L1** in THF (Fig. 2) displays a strong band with maximum at 622 nm and a shoulder around 650–660 nm. A very similar spectrum is seen for the brominated ligand **L2**, the only differences being a small red shift to 624 nm and a decrease in intensity. The fluorescence quantum yields of the ligands were determined in THF by comparison with chlorophyll A in ether solution. They amount to 31 and 21%, respectively, that is Φ_F decreases by about one third

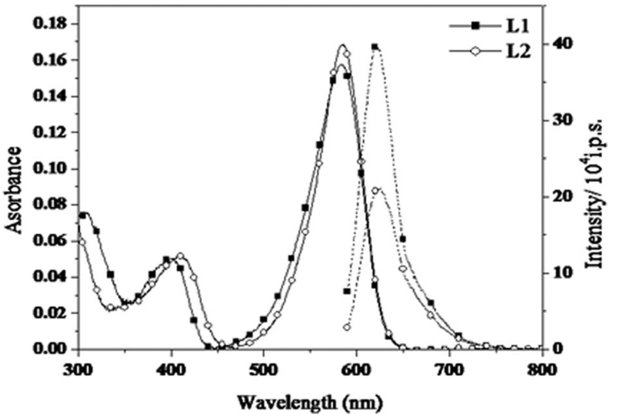

Fig. 2 Absorption (left) and photoluminescence (right; λ_{exc} = 583 nm) spectra of the Bodipy ligands with the concentration of 1.0×10^{-5} M in THF.

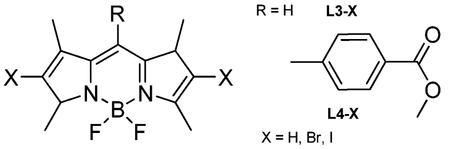

Scheme 2 Halogenated Bodipy compounds from the literature: **L3-X**[27] and **L4-X.**[29]

upon bromination of **L1**. Preparation of halogenated Bodipy derivatives **L3-X** and **L4-X** (Scheme 2, X = H, Br, I) has been previously reported.[27,29] In both cases, halogenation of the 2,6 positions led to a red-shift of the fluorescence band up to 30–40 nm, reduction in fluorescence lifetime, and decrease in the fluorescence quantum yield. This has been explained by an increase in the isc rate constant attributable to the heavy atom effect. For **L3-X** ligands (X = H, Br), which were designed for PDT of cancer, the consequence is an increase in the yield of $^1O_2$,[27] for **L4-X** compounds (X = H, Br, I), very weak bands at around 800 nm were detected at room temperature, with lifetimes in the ms range, assigned to triplet states.[29]

To determine whether the bromo-substituted ligand **L2** displays phosphorescence or not, we have measured the emission of both ligands in N_2-saturated 2-methyl-THF at room temperature and 77 K under fluorescence (Fig. 3, top) and phosphorescence (Fig. S11 in ESI†) conditions. An intense band is seen at room temperature for each ligand. Gaussian decomposition reveals main maxima at 623 (**L1**) and 627 (**L2**) nm and additional components at 678 (**L1**) and 680 (**L2**) nm, respectively. When solutions of the ligands are saturated with di-oxygen, no luminescence from singlet oxygen is detected around 1.25 μm. At liquid nitrogen temperature, the corresponding data are similar, 621, 683 (**L1**) and 624, 687 (**L2**) nm, but the low energy component is much more intense. When a time delay is enforced the signals disappear completely at both temperatures (Fig. S11 in ESI†). At room temperature, decays of the fluorescence maxima can be fitted with single exponential functions, yielding lifetimes of 1.0 and 0.6 ns for **L1** and **L2**, respectively. At 77 K, lifetimes associated with the decays monitored at 626 and 711 nm are in the range 5–6 ns for **L1** and 3.9–4.3 ns for **L2**, comparable to the lifetimes reported for **L4-H** (2.9 ns) and **L4-Br** (1.3 ns).[29] Therefore both components are fluorescence bands, the second one being probably a vibronic component since the energy difference between the two maxima is 1240–1300 cm^{-1} at room temperature and 1400–1450 cm^{-1} at 77 K, corresponding to a ring-breathing vibrational mode.

A similar situation is met for the Gd^{III} complexes but the emission spectra are broadened rendering Gaussian decomposition difficult (Fig. 3, bottom). The main difference is a very large enhancement of the low energy component at 77 K, red shifted at 1300–1550 cm^{-1} with respect to the high energy component, as well as the appearance of a weak shoulder at around 750 nm. However, enforcing a time delay results again in a total loss of the signal (Fig. S12 in ESI†). The luminescence decays of both components are bi-exponential at room temperature with a short component (~0.6–1 ns) and a longer one (2.4–3.1 ns) corresponding to a population of ~10%. At 77 K, the decays become monoexponential with a lifetime of 5–6 ns (**GdL1**) and 3.7–4.0 ns (**GdL2**). Finally, closer scrutiny of all spectra in the range 700–850 nm did not reveal any

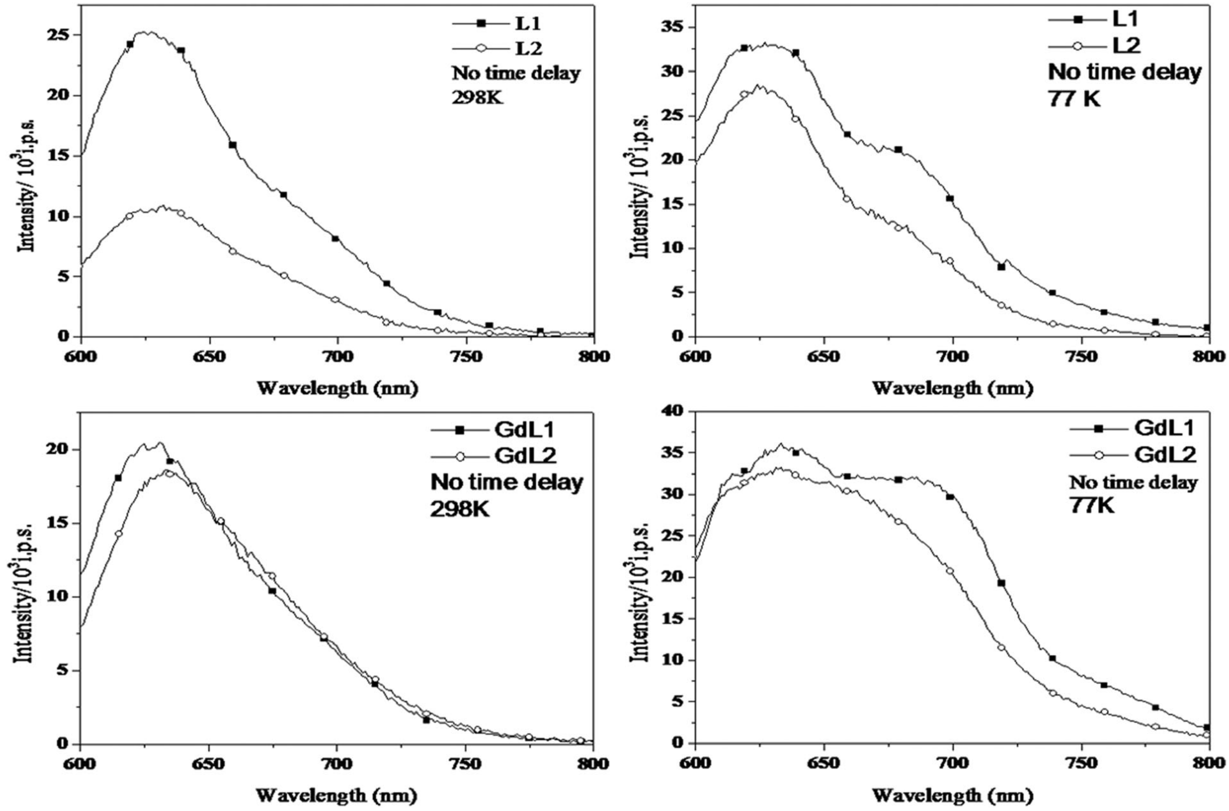

Fig. 3 Fluorescence spectra of the ligands (top) and Gd^{III} complexes (bottom) in 2-methyl THF at room temperature (left) and 77 K (right).

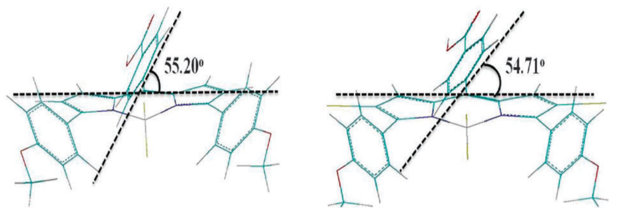

Fig. 4 Snapshots of the calculated structures of **L1** (left) and **L2** (right) at the AM1 level.

genuine emission band that could be assigned to triplet state emission, even for the Gd^{III} complex with brominated ligand **L2**, pointing to no or small heavy atom effect and/or fast de-activation of the triplet state. We note, however, that triplet state emission can be very weak in Bodipy ligands[29] and that it occurs in a spectral range in which our detector is not very sensitive. As a comparison, very weak triplet state emission from Bodipy has been evidenced at 77 K around 730 nm in an Ir^{III} complex with an ethynyl derivatized Bodipy. The associated lifetime of the ^{3}IL state is 25 μs.[35] In the latter compound, the Bodipy moiety adopts a planar conformation, which is not the case for ligands **L1** and **L2** (Fig. 4).

Metal-centered NIR luminescence

The Ln^{III}-cored Bodipy complexes, Ln**L***i*, display UV-Vis absorption and ligand emission behaviors similar to the unbound ligands (Fig. 5 and Table 1). Upon photo-excitation at the wavelength corresponding to the absorption maximum of the ligands, the intensity of the ligand emission remains unchanged for **GdL1** (within experimental errors) and is slightly smaller for **GdL2** (−8%) while it is noticeably reduced for the Er^{III} and Yb^{III} complexes. The decrease is the same (∼−30%) for the complexes with **L1** while being differentiated for the complexes with **L2**: −40% for Er^{III} and −20% for Yb^{III}. Lifetime measurements in *m*-THF confirm data reported above for **GdL*i***: decays are biexponential at room temperature with the longest component (2.4–3.5 ns) accounting for about 5–15% of the population while they become mono-exponential at 77 K with lifetime comparable to those of the Gd^{III} complexes. In parallel, typical, although weak, metal-centered emission of the Er^{III} and Yb^{III} ions is observed with maxima about 1530 and 978 nm, respectively (Fig. 6). The emission band of Er^{III} is ascribed to the 4f–4f electronic transition originating from the first excited state ($^4I_{13/2}$) to the ground state ($^4I_{15/2}$) and the emission of the Yb^{III} complexes to the $^2F_{5/2} \rightarrow {}^2F_{7/2}$ transition. Excitation spectra clearly match the absorption spectra (Fig. S13 in ESI†). All these data point to energy transfer operating between the ligands and the NIR-emitting Ln^{III} ions. From data reported in Table 1 one can estimate the fraction ($1 - I_{Ln}/I_{Gd}$) of energy transferred onto the

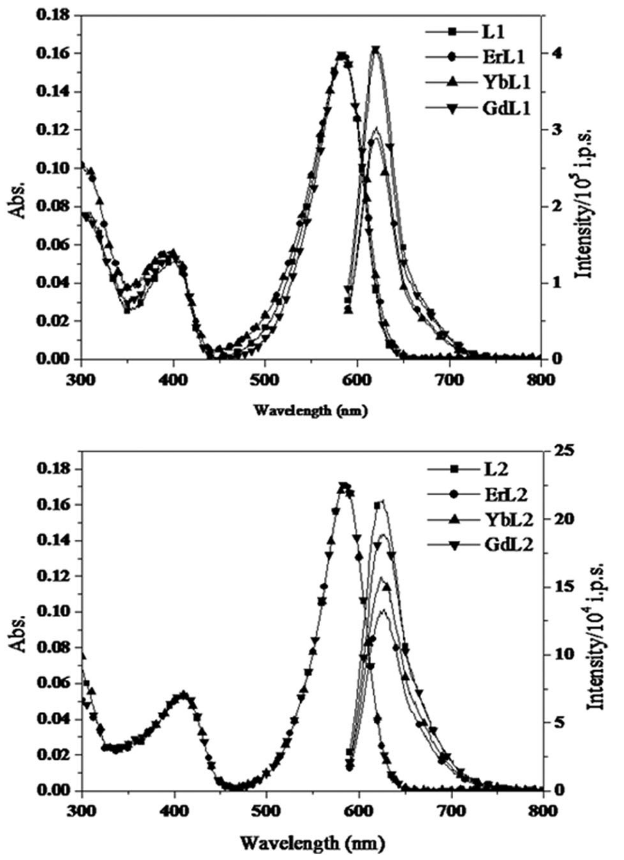

Fig. 5 Absorption (up) and emission (bottom) spectra of **L*i*** (*i* = 1, 2) and **LnL*i*** complexes in THF at room temperature; measured at constant absorbance, [**L*i***] ≈ 3.0 × 10^{-6} M and [**LnL*i***] ≈ 1.0 × 10^{-6} M.

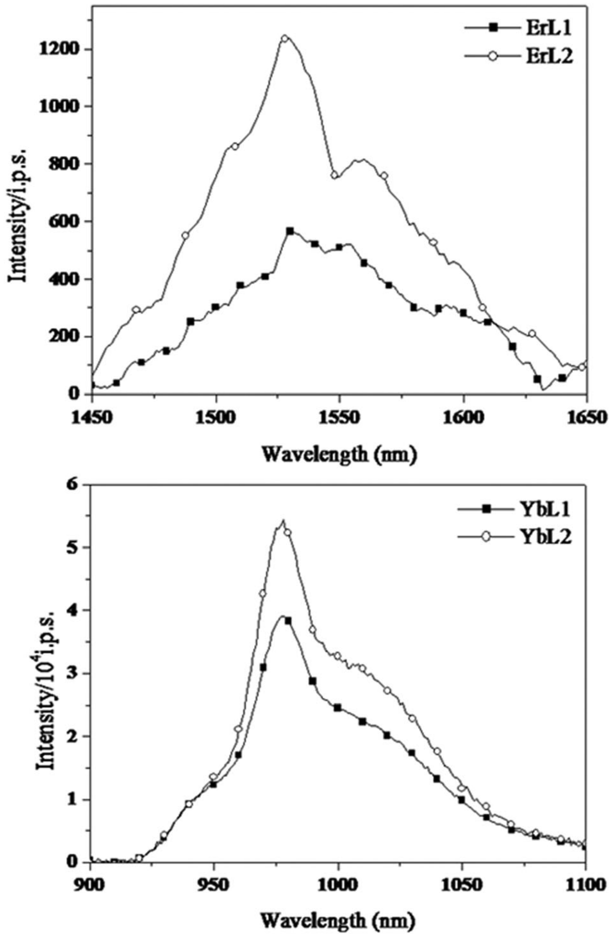

Fig. 6 Metal-centred NIR emission of **ErL*i*** (up) and **YbL*i*** (bottom) with the concentration of 1 × 10^{-5} M in THF at room temperature; λ_{ex} = 583 nm.

Table 2 Emission characteristics of the **LnL*i*** complexes measured at constant absorbance in THF at room temperature

Compound	λ_{em}/nm	I_{int}	I_{int}(rel)
ErL1	1530	1237	1.0
ErL2	1530	565	0.46
YbL1	978	54 335	1.0
YbL2	978	39 110	0.72

metal ion as being 25–29% for complexes with **L1**, 32% for **ErL2**, but only 17% for **YbL2**. In reality, both complexes with **L2** are less luminescent than those with **L1**. Comparing solutions with the same complex concentration (1×10^{-5} M) shows that the NIR emission intensity of **ErL1** is enhanced about 2-fold compared to the fluorescence of **ErL2** while the enhancement is a factor 1.4 for **YbL1** with respect to **YbL2** (Table 2).

The efficiency of energy transfer between ligands and metal ions is primarily controlled by two parameters: (i) the position (distance and orientation) of the energy-donor chromophores with respect to the acceptor ion and (ii) the spectral overlap between the emission spectrum of the donor and the absorption spectrum of the acceptor. This overlap is shown in Fig. 7 for **L1** and Er^{III}: the emission band of the ligand occurs at the same energy as the $^4F_{9/2} \leftarrow {}^4I_{15/2}$ transition so that sensitization may be expected even if the overlap integral is small. Possible energy-transfer pathways for the sensitized emission in luminescent lanthanide complexes involve different ligand and metal-ion states. A common path is energy transfer through the triplet state of the photoexcited luminescent ligand after suitable conversion from the excited singlet state *via* intersystem crossing. This path is usually reinforced when a heavy-atom effect is operating. In our case, we have been unable to locate the triplet state of the ligands even in the Gd^{III} complexes despite the presence of two bromine substituents on **L2**. We trace back the absence of phosphorescence to the dihedral angle between the phenyl groups and the dipyrromethene unit which amounts to ~55°, leading to less conjugation between the phenyl moiety and the π-extended dipyrromethene unit. It is worth pointing out that the calculated dihedral angle of the ligands is consistent with the absorption spectra which exhibit three maxima in THF at 300–310 nm, 400 nm and 583–584 nm, corresponding to transitions located on the phenyl groups for the former one and the π-extended dipyrromethene unit for two latter ones Thus, phosphorescence is not detected because the restricted rotation between the phenyl and dipyrromethene units may prevent heavy atom effect (Fig. 4). Therefore we postulate that the energy-transfer pathway for the sensitization of the NIR-emitting LnL*i* complexes mainly involves singlet excited states. It is not clear though why **L2** leads to sensitizaton efficiencies which are much less good (−40 to −100%) than those induced by **L1** whereas its energy levels are very comparable and quantum yield is only ~30% smaller. A detailed study for elucidating this trend would involve fast time-resolved spectroscopy to which we have presently no access.

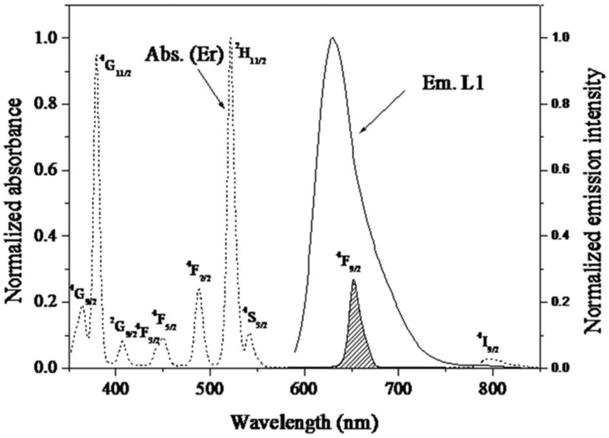

Fig. 7 Spectral overlap between the absorption spectrum of $ErCl_3$ in THF and the emission spectrum of **L1** in THF.

Conclusions

Although initially designed for testing the singlet *versus* triplet state pathway for the sensitization of NIR-emitting Ln^{III} ions, ligands **L1** and **L2** proved to behave similarly in that intersystem crossing is negligible for both of them as well as for the corresponding Ln^{III} complexes. Therefore sensitization of the Er^{III}- and Yb^{III}-cored complexes is postulated to be achieved through the lowest $^1\pi\pi$ state which is in resonance with the $^4F_{9/2}$ level of the former ion while the energy difference with the $Yb(^2F_{5/2})$ excited level amounts to 5700 cm^{-1}, a not too large gap for energy transfer. The experimental evidences reported here point to the Bodipy framework being adequate for transferring energy onto NIR-emitting Ln^{III} ions, with excitation in the orange region of the visible spectrum; in addition the complexes have high molar absorption coefficients ($\log \varepsilon \approx 5.0$–$5.2$). While remaining modest, the amount of energy transferred from the ligands (20–40%) is sizeable; the weak metal-centered luminescence observed at room temperature is mainly due to deactivation through high-energy vibrations, which explains why Er^{III} complexes are less luminescent than their Yb^{III} counterparts, as observed for complexes with a 8-hydroxyquinoline-derivatized Bodipy ligand.[37]

For a more efficient sensitization, the present framework will have to be modified in order to render it more planar so that intersystem crossing can be induced by the heavy atom effect; moreover, non-radiative de-activations will have to be minimized by halogenation. Work is in progress in our laboratory toward these goals.

Acknowledgements

This research was supported by a grant from the Fundamental R&D Program for Core Technology of Materials funded by the Ministry of Knowledge Economy, WCU Center for Next Generation Photovoltaic System (The Ministry of Education and Science, grant R31-2008-000-10035-0), and by a grant from Korea University (2010).

References

1 L. D. Carlos, R. A. S. Ferreira, V. de Zea Bermudez, B. Julian-Lopez and P. Escribano, *Chem. Soc. Rev.*, 2011, **40**, 536.
2 S. V. Eliseeva and J.-C. G. Bünzli, *New J. Chem.*, 2011, **35**, 1165.
3 J.-C. G. Bünzli and S. V. Eliseeva, *J. Rare Earths*, 2010, **28**, 824.
4 R. A. S. Ferreira, P. S. André and L. D. Carlos, *Opt. Mater. (Amsterdam)*, 2010, **32**, 1397.

5 H. K. Kim, J. B. Oh, N. S. Baek, S. G. Roh, M. K. Nah and Y. H. Kim, *Bull. Korean Chem. Soc.*, 2005, **26**, 201.
6 H. K. Kim, S. G. Roh, K. S. Hong, J. W. Ka, N. S. Baek, J. B. Oh, M. K. Nah, Y. H. Cha and J. Ko, *Macromol. Res.*, 2003, **11**, 133.
7 J. H. Oh, H. M. Song, Y. K. Eom, J. H. Ryu, M. J. Ju and H. K. Kim, *Bull. Korean Chem. Soc.*, 2011, **32**, 2743.
8 M. P. O. Wolbers, F. C. J. M. Van Veggel, F. G. A. Peters, E. S. E. Van Beelen, J. W. Hofstraat, F. A. J. Geurts and D. N. Reinhoudt, *Chem.–Eur. J.*, 1998, **4**, 772.
9 J. Kido and Y. Okamoto, *Chem. Rev.*, 2002, **102**, 2357.
10 S. V. Eliseeva and J.-C. G. Bünzli, *Chem. Soc. Rev.*, 2010, **39**, 189.
11 E. S. Andreiadis, R. Demadrille, D. Imbert, J. Pecaut and M. Mazzanti, *Chem.–Eur. J.*, 2009, **15**, 9458.
12 J. E. Jones and S. J. A. Pope, *Dalton Trans.*, 2009, 8421.
13 N. M. Shavaleev, R. Scopelliti, F. Gumy and J.-C. G. Bünzli, *Inorg. Chem.*, 2009, **48**, 6178.
14 M. Kleinerman, *J. Chem. Phys.*, 1969, **51**, 2370.
15 A. P. Souza, L. C. V. Rodrigues, H. F. Brito, S. Alves and O. L. Malta, *J. Lumin.*, 2010, **130**, 181.
16 M. H. Ha-Thi, J. A. Delaire, V. Michelet and I. Leray, *J. Phys. Chem. A*, 2009, **114**, 3264.
17 S. G. Roh, N. S. Baek, Y. H. Kim and H. K. Kim, *Bull. Korean Chem. Soc.*, 2007, **28**, 1249.
18 V. F. Zolin, L. N. Puntus, V. I. Tsaryuk, V. A. Kudryashova, J. Legendziewicz, P. Gawryszewska and R. Szostak, *J. Alloys Compd.*, 2004, **380**, 279.
19 A. Vogler and H. Kunkely, *Inorg. Chim. Acta*, 2006, **359**, 4130.
20 Y. H. Kim, N. S. Baek and H. K. Kim, *ChemPhysChem*, 2006, **7**, 213.
21 N. M. Shavaleev, R. Scopelliti, F. Gumy and J.-C. G. Bünzli, *Inorg. Chem.*, 2009, **48**, 7937.
22 J. B. Oh, Y. H. Kim, M. K. Nah and H. K. Kim, *J. Lumin.*, 2005, **111**, 255.
23 N. S. Baek, Y. H. Kim, S. G. Roh, B. K. Kwak and H. K. Kim, *Adv. Funct. Mater.*, 2006, **16**, 1873.
24 M. K. Nah, H. G. Cho, H. J. Kwon, Y. J. Kim, C. Park, H. K. Kim and J. G. Kang, *J. Phys. Chem. A*, 2006, **110**, 10371.
25 G. Ulrich, R. Ziessel and A. Harriman, *Angew. Chem., Int. Ed.*, 2008, **47**, 1184.
26 S. L. Niu, C. Massif, G. Ulrich, R. Ziessel, P. Y. Renard and A. Romieu, *Org. Biomol. Chem.*, 2011, **9**, 66.
27 T. Yogo, Y. Urano, Y. Ishitsuka, F. Maniwa and T. Nagano, *J. Am. Chem. Soc.*, 2005, **127**, 12162.
28 T. Rousseau, A. Cravino, T. Bura, G. Ulrich, R. Ziessel and J. Roncali, *Chem. Commun.*, 2009, 1673.
29 R. P. Sabatini, T. M. McCormick, T. Lazarides, K. C. Wilson, R. Eisenberg and D. W. McCamant, *J. Phys. Chem. Lett.*, 2011, **2**, 223.
30 L. W. Knight, J. W. Huffman and M. L. Isherwood, *Synlett*, 2003, 1993.
31 E. Spinner, *J. Chem. Soc. B*, 1967, 874.
32 S.-G. Roh, N. S. Baek, K.-S. Hong and H. K. Kim, *Bull. Korean Chem. Soc.*, 2004, **25**, 343.
33 A. Dupraz, P. Guy and C. Dupuy, *Tetrahedron Lett.*, 1996, **37**, 1237.
34 J. Karolin, L. B. A. Johansson, L. Strandberg and T. Ny, *J. Am. Chem. Soc.*, 1994, **116**, 7801.
35 A. A. Rachford, R. Ziessel, T. Bura, P. Retailleau and F. N. Castellano, *Inorg. Chem.*, 2010, **49**, 3730.
36 G. Weber and F. W. J. Teale, *Trans. Faraday Soc.*, 1957, **53**, 646.
37 R. Ziessel, G. Ulrich, L. J. Charbonnière, D. Imbert, R. Scopelliti and J.-C. G. Bünzli, *Chem.–Eur. J.*, 2006, **12**, 5060.